

## Photoredox-Catalyzed Cyclopropanation via Ligated Boryl Radical-Mediated Nonstabilized Carbene Formation

Rong-Bin Liang, Chao Yang, Wujiong Xia, and Lin Guo\*

Cite This: <https://doi.org/10.1021/jacs.5c12677>

Read Online

ACCESS |



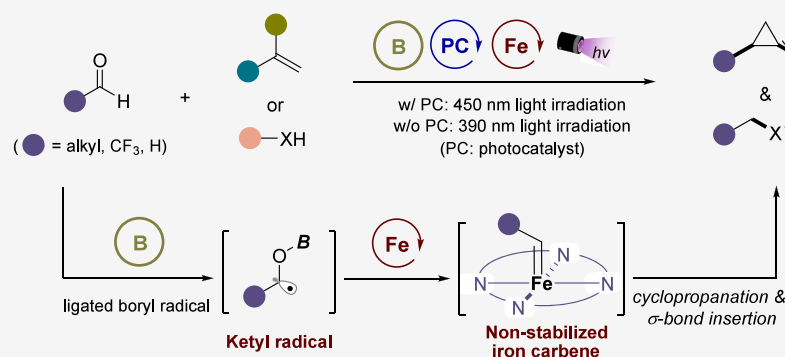
Metrics &amp; More



Article Recommendations



Supporting Information



**ABSTRACT:** The [2 + 1] cycloaddition of carbenes with alkenes is widely regarded as one of the most straightforward strategies for synthesizing cyclopropanes, which are ubiquitous motifs in pharmaceuticals. A significant challenge in cyclopropanation reactions is managing the high reactivity and inherent safety risks associated with the use of diazo compounds, particularly alkyl-substituted variants, as carbene precursors. Leveraging metallaphotoredox catalysis, we report the development of a method for ligated boryl radical-mediated generation of nonstabilized metal carbenes directly from aliphatic aldehydes. Employing  $B_2cat_2$  as the activating agent for the carbonyl group, this approach enables the direct use of alkyl aldehydes as nonstabilized carbene precursors, eliminating the need for substrate prefunctionalization. This protocol features mild conditions, broad substrate scope (>88 examples), and good functional group tolerance, demonstrating its applicability in diverse cyclopropanation and  $\sigma$ -bond insertion reactions. Preliminary mechanistic studies have been also performed to elucidate the reaction pathway.

## 1. INTRODUCTION

The cyclopropane scaffold is a key pharmacophore found in many drug molecules and biologically active natural products.<sup>1</sup> The rigid structure of cyclopropane enhances binding to biological targets by reducing molecular flexibility, enabling it to serve as a bioisostere for alkyl and aryl substitutions while conferring resistance to oxidative metabolism in drug molecules.<sup>2</sup> Figure 1a illustrates representative pharmaceuticals containing the cyclopropane core structure, which exhibit varied pharmacological activities. Consequently, the significance of cyclopropane as a medicinally privileged scaffold has driven the development of efficient synthetic methods for rapid and diverse access. Among current synthetic approaches to cyclopropane units, [2 + 1] cycloaddition of carbenes and alkenes is widely regarded as one of the most efficient and straightforward strategies.<sup>3</sup> Despite significant progress in this field, most synthetic protocols rely on diazo compounds as carbene precursors—species that are highly reactive and present inherent safety risks due to potential explosive decomposition and uncontrolled chain reactions.<sup>4</sup> Advances in carbene chemistry over recent decades have driven the development of numerous strategies, particularly the use of

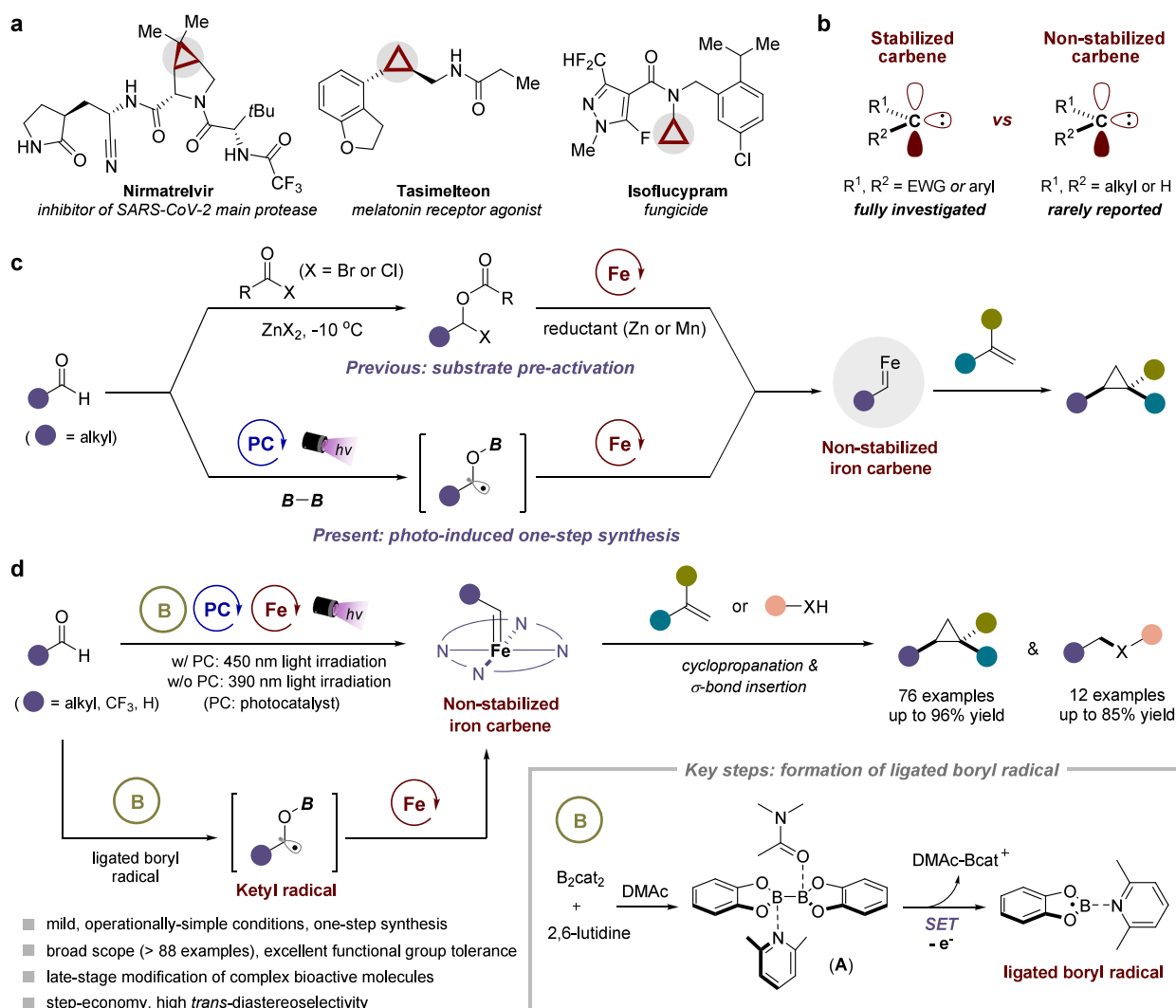
stabilized carbene precursors bearing resonance stabilizing groups (e.g., electron-withdrawing groups or aryl substituents), enabling safe preparative-scale applications.<sup>5</sup> In contrast, since alkyl-substituted diazo compounds exhibit extreme susceptibility to exothermic spontaneous decomposition,<sup>4</sup> the employment of these nonstabilized carbene precursors requires *in situ* generation,<sup>6</sup> especially via continuous-flow techniques (Figure 1b).<sup>7</sup> Although recent advances have achieved some success in cyclopropanation reactions by the manipulation of non-stabilized carbenes from other precursors, including gem-dihalides, hydrazones and sulfones instead of highly reactive diazo compounds, the complexity of carbene precursor preparation and narrow applicability still constrain the development of these reactions.<sup>8</sup> The development of new methods for converting simple, stable, and easily available

Received: July 24, 2025

Revised: September 18, 2025

Accepted: September 19, 2025






**Figure 1.** Inspiration and design for metallaphotoredox-catalyzed cyclopropanation. (a) Cyclopropane motif in molecular drugs. (b) Comparison between stabilized and nonstabilized carbenes. (c) Cyclopropanation with nonstabilized iron carbenes generated from aldehydes. (d) This work.

feedstocks into functionalized cyclic skeletons under mild conditions remains a formidable challenge.

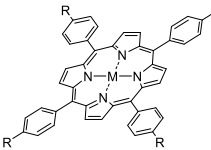
Carbonyl compounds are fundamental substrates in organic synthesis, and developing strategies to functionalize aliphatic carbonyl derivatives represents a frontier of significant interest. By circumventing traditional reliance on highly reactive diazo compounds, direct activation of aliphatic aldehydes enables a paradigm shift for in situ carbene generation—transforming abundant feedstocks into valuable intermediates.<sup>9</sup> Not surprisingly, recent years have witnessed elegant approaches to the cyclopropanation reactions from aliphatic aldehydes. Nagib and co-workers achieved a breakthrough by describing multistep access to nonstabilized metal carbenes via stable  $\alpha$ -acyloxy halide intermediates.<sup>10</sup> This strategy enables safe handling and reactivity of nonstabilized carbenes (from alkyl, aryl, and formyl aldehydes) through zinc carbenoid<sup>10a,c</sup> or ketyl radical intermediates,<sup>10d</sup> facilitating versatile cyclopropanation reactions with diverse alkenes (Figure 1c, upper panel). However, aliphatic aldehydes require low-temperature pre-activation to form reactive  $\alpha$ -acyloxy halide intermediates, while superstoichiometric quantities of zinc/manganese as strong metal reductants are needed to generate nonstabilized carbenes. The related one-step direct carbonyl activation to

access carbene intermediates still remains unreported. Nonetheless, such a synthetic strategy would significantly expand the scope of carbene chemistry by avoiding the strongly reducing conditions of the single-electron reduction pathway, and circumventing the acyl halide activators needed for  $\alpha$ -acyloxy halide-mediated carbene generation (Figure 1c, lower panel).

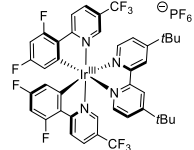
Recent years have seen rapid advancements in visible light photocatalysis, a technique that utilizes visible light as a clean energy source.<sup>11</sup> The use of photoredox catalysis has led to significant progress in the catalytic generation of ketyl radicals via single electron transfer (SET) reduction, which inverts the inherent polarity of carbonyl group, converting electrophilic centers into nucleophilic radicals.<sup>12</sup> Strategies like proton-coupled electron transfer (PCET)<sup>13</sup> and carbonyl-metal complexation<sup>14</sup> successfully access ketyl radicals, yet remain largely limited to easily reducible aromatic carbonyls. Aliphatic carbonyl activation and functionalization still remains challenging due to their high reduction potentials.<sup>15</sup> To overcome this limitation and extend the scope to aliphatic carbonyls, we envisioned a direct activation strategy using organoboron compounds to directly generate ketyl radicals from aldehydes (Figure 1d). Initial addition of diboron with pyridine derivative in DMAc forms redox-active complex (A),<sup>16</sup> which undergoes

Table 1. Optimization Studies<sup>a</sup>


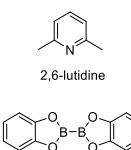
entry	deviation from the above condition	c-19 (%) <sup>b</sup>	d.r. <sup>c</sup>
1	none	90	6.9:1
2	Et3N instead of 2,6-lutidine	51	7.6:1
3	2,4,6-collidine instead of 2,6-lutidine	75	5.2:1
4	DMAP instead of 2,6-lutidine	35	5.5:1
5	iPr2NEt instead of 2,6-lutidine	55	7.9:1
6	ZnBr2, ZnCl2, FeCl3, TMSCl, or B2pin2 instead of B2cat2	N.D.	-
7	Fe(TPP)Cl instead of Fe(TMPP)Cl	69	7.0:1
8	Co(TPP) instead of Fe(TMPP)Cl	N.D.	-
9	Cu(TMPP) instead of Fe(TMPP)Cl	N.D.	-
10	FeCl2·4H2O instead of Fe(TMPP)Cl	N.D.	-
11	without photocatalyst	trace	-
12 <sup>d</sup>	without photocatalyst, using 390 nm purple LED (10 W)	60	6.0:1
13	without B2cat2, Fe(TMPP)Cl, or light irradiation	N.D.	-



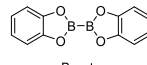
M = Fe, Co, Cu  
TPP (R = H), TMPP (R = OMe)



[Ir(dFCF<sub>3</sub>ppy)<sub>2</sub>(dtbbpy)]PF<sub>6</sub>



2,6-lutidine



B<sub>2</sub>cat<sub>2</sub>

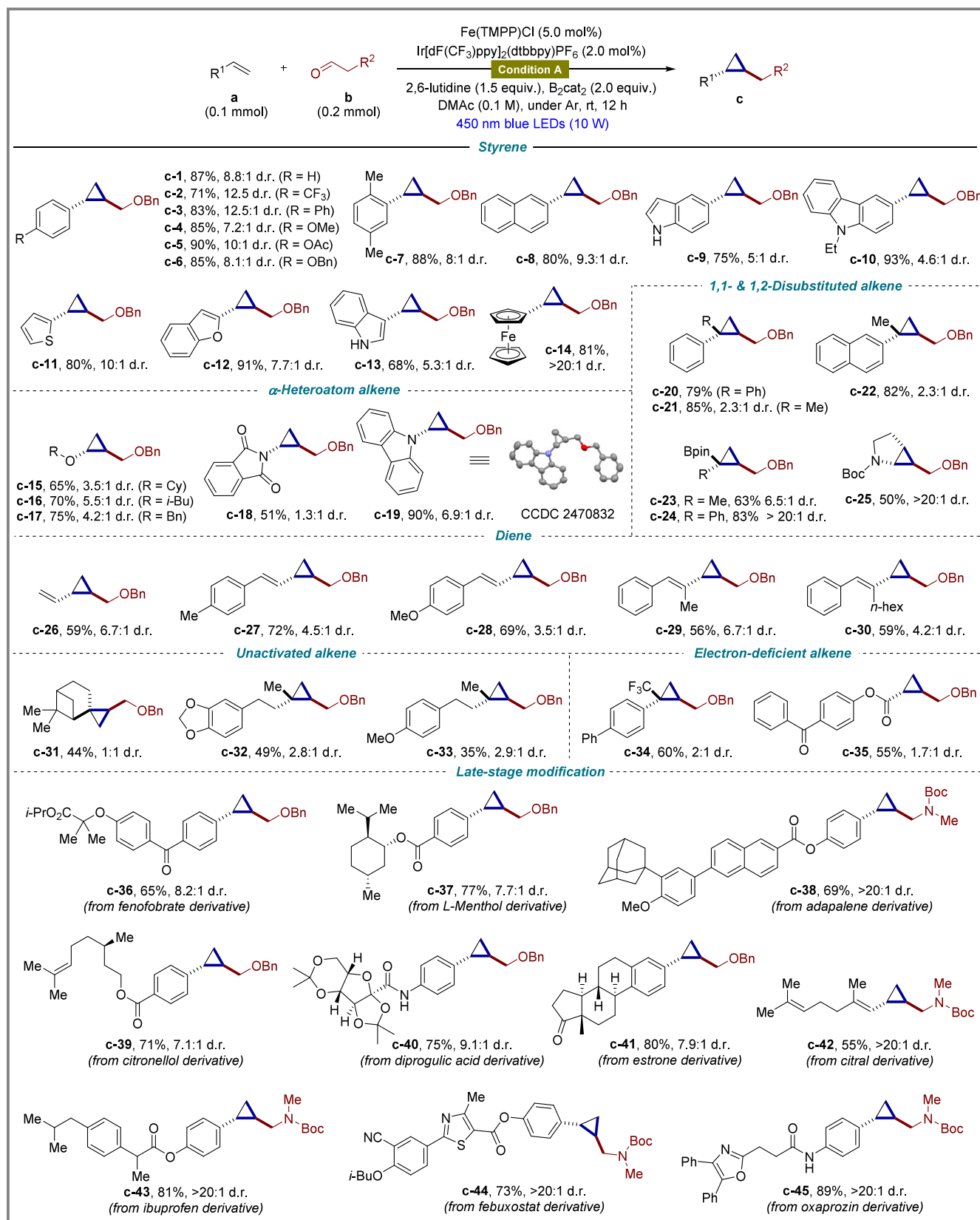
<sup>a</sup>Reaction conditions: **a-19** (0.1 mmol, 1.0 equiv), **b-1** (0.2 mmol, 2.0 equiv), Ir(dFCF<sub>3</sub>ppy)<sub>2</sub>(dtbbpy)PF<sub>6</sub> (2.0 mol %), 2,6-lutidine (0.15 mmol, 1.5 equiv), B<sub>2</sub>cat<sub>2</sub> (0.2 mmol, 2.0 equiv), Fe(TMPP)Cl (5.0 mol %) in DMAc (1.0 mL, 0.1 M) at room temperature, under Ar atmosphere, 450 nm LEDs (10 W), 12 h. <sup>b</sup>Yields of isolated products after chromatographic purification. <sup>c</sup>Diastereomeric ratio (d.r.) determined by <sup>1</sup>H NMR (*trans*:*cis*). <sup>d</sup>DMAc:acetone = 1:1 (1.0 mL, 0.1 M). N.D. = Not detected.

SET-mediated boron–boron bond cleavage to release a ligated boryl radical. This reactive intermediate enables carbonyl addition to form ketyl radicals,<sup>17</sup> facilitating subsequent radical addition to iron-porphyrin complex<sup>18</sup> and  $\alpha$ -oxy elimination to furnish the desired nonstabilized iron carbene species.<sup>19</sup> Herein, we report the successful development of this metallaphotoredox-catalyzed strategy for ligated boryl radical-mediated nonstabilized metal carbene formation directly from aliphatic aldehydes and demonstrate its application in cyclopropanation and  $\sigma$ -bond insertion reactions (Figure 1d). It is important to note that this novel approach utilizes iridium-based photocatalyst under 450 nm visible light irradiation to facilitate the SET-mediated carbonyl reduction, and circumvents the strongly reducing conditions required for traditional reductive ketyl radical formation. Alternatively, cyclopropanation reaction also proceeds efficiently under 390 nm light irradiation without external photocatalyst, as the in situ formed diboron-pyridine adduct (**A**) could undergo direct photoexcitation to initiate the SET process.<sup>20</sup>

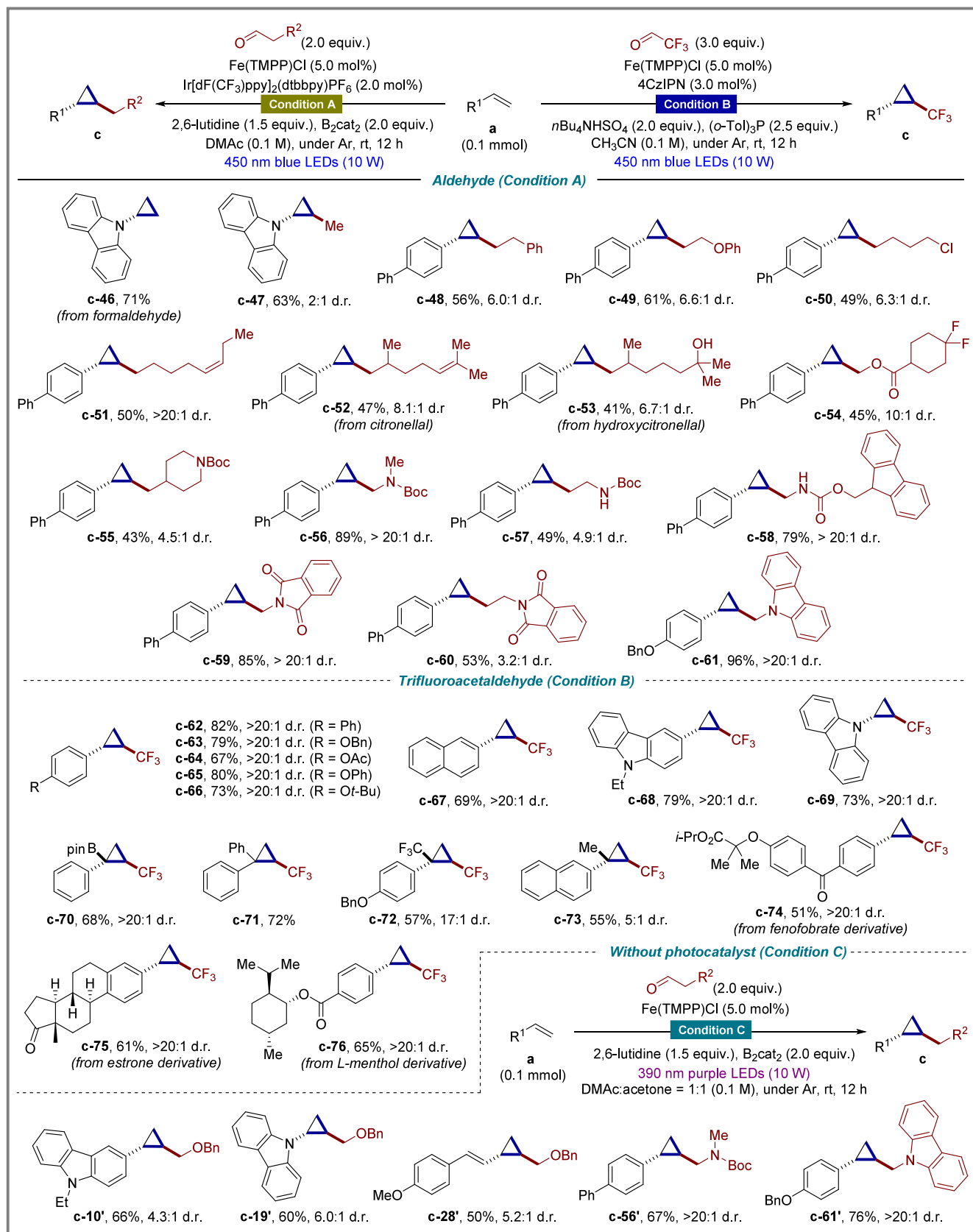
## 2. RESULTS AND DISCUSSION

To validate our hypothesis, we initiated our investigations by using *N*-vinylcarbazole (**a-19**) and benzoyloxyacetaldehyde (**b-1**) as model substrates in the presence of an iridium-based photocatalyst and iron(III)-porphyrin complex. After extensive screening of the reaction conditions, it is encouraging to observe that the expected cyclopropanation of alkene did occur to give the desired product **c-19** in 90% isolated yield with

6.9:1 diastereomeric ratio (*trans*:*cis*), supporting our hypothesis of metallaphotoredox-catalyzed nonstabilized carbene generation (Table 1, entry 1). Screenings of different bases showed 2,6-lutidine to be the most effective (entries 2–5). Despite extensive screening of alternative Lewis acids including ZnBr<sub>2</sub>, ZnCl<sub>2</sub>, FeCl<sub>3</sub>, TMSCl, or B<sub>2</sub>pin<sub>2</sub> in place of bis(catecholato)diboron (B<sub>2</sub>cat<sub>2</sub>), no detectable formation of the desired product **c-19** was observed (entry 6), which revealed the crucial role of B<sub>2</sub>cat<sub>2</sub> in activating the carbonyl group of aldehyde substrate and facilitating the iron carbene formation. In addition, replacing the Fe(TMPP)Cl catalyst with Fe(TPP)Cl resulted in a decreased yield to 69% (entry 7), while no desired product was observed if Co(TPP), Cu(TMPP), or FeCl<sub>2</sub>·4H<sub>2</sub>O was employed instead of Fe(TMPP)Cl (entries 8–10).<sup>21</sup> Intriguingly, conducting the photoinduced reaction in the absence of iridium-based photocatalyst, Ir(dFCF<sub>3</sub>ppy)<sub>2</sub>(dtbbpy)]PF<sub>6</sub>, yielded **c-19** in only trace amount, whereas substituting blue LEDs ( $\lambda$  = 450–455 nm) with a 390 nm light source ( $\lambda$  = 390–395 nm) resulted in a substantial increase in reaction efficiency, suggesting a distinct activation pathway under purple light irradiation (entries 11–12).<sup>20b,22</sup> Although Fe(TMPP)Cl catalyst also exhibits visible light absorption at both 450 and 390 nm, the above results indicated that Fe(TMPP)Cl did not act as a photocatalyst to carry out the single electron transfer process. At last, control experiments confirmed that B<sub>2</sub>cat<sub>2</sub>, Fe(TMPP)Cl, and light irradiation are all essential for the desired transformation (entry 13).

Scheme 1. Substrate Scope of Alkene<sup>a</sup>

<sup>a</sup>Conditions A: alkene **a** (0.1 mmol, 1.0 equiv), aldehyde **b** (0.2 mmol, 2.0 equiv), Ir[dFCF<sub>3</sub>ppy]<sub>2</sub>(dtbbpy)PF<sub>6</sub> (2.0 mol %), 2,6-lutidine (0.15 mmol, 1.5 equiv), B<sub>2</sub>cat<sub>2</sub> (0.2 mmol, 2.0 equiv), Fe(TMPP)Cl (5.0 mol %) in DMAc (1.0 mL, 0.1 M) at room temperature, under Ar atmosphere, 450 nm LEDs (10 W), 12 h. Yields of isolated products after chromatographic purification. Diastereomeric ratio (d.r.) determined by <sup>1</sup>H NMR (*trans:cis*).

Scheme 2. Substrate Scope of Aldehyde and Trifluoromethyl Cyclopropane<sup>a</sup>

<sup>a</sup>Conditions A: alkene **a** (0.1 mmol, 1.0 equiv.), aldehyde **b** (0.2 mmol, 2.0 equiv.), Ir[dFCF<sub>3</sub>ppy]<sub>2</sub>(dtbbpy)PF<sub>6</sub> (2.0 mol %), 2,6-lutidine (0.15 mmol, 1.5 equiv.), B<sub>2</sub>cat<sub>2</sub> (0.2 mmol, 2.0 equiv.), Fe(TMPP)Cl (5.0 mol %) in DMAc (1.0 mL, 0.1 M) at room temperature, under Ar atmosphere, 450 nm LEDs (10 W), 12 h. Conditions B: alkene **a** (0.1 mmol, 1.0 equiv.), trifluoroacetaldehyde **b** (0.3 mmol, 3.0 equiv.), 4CzIPN (3.0 mol %), *n*Bu<sub>4</sub>NHSO<sub>4</sub> (0.2 mmol, 2.0 equiv.), (*o*-Tol)<sub>3</sub>P (tri(*o*-tolyl)phosphine, 0.25 mmol, 2.5 equiv.), Fe(TMPP)Cl (5.0 mol %) in CH<sub>3</sub>CN (1.0 mL, 0.1



## Scheme 2. continued

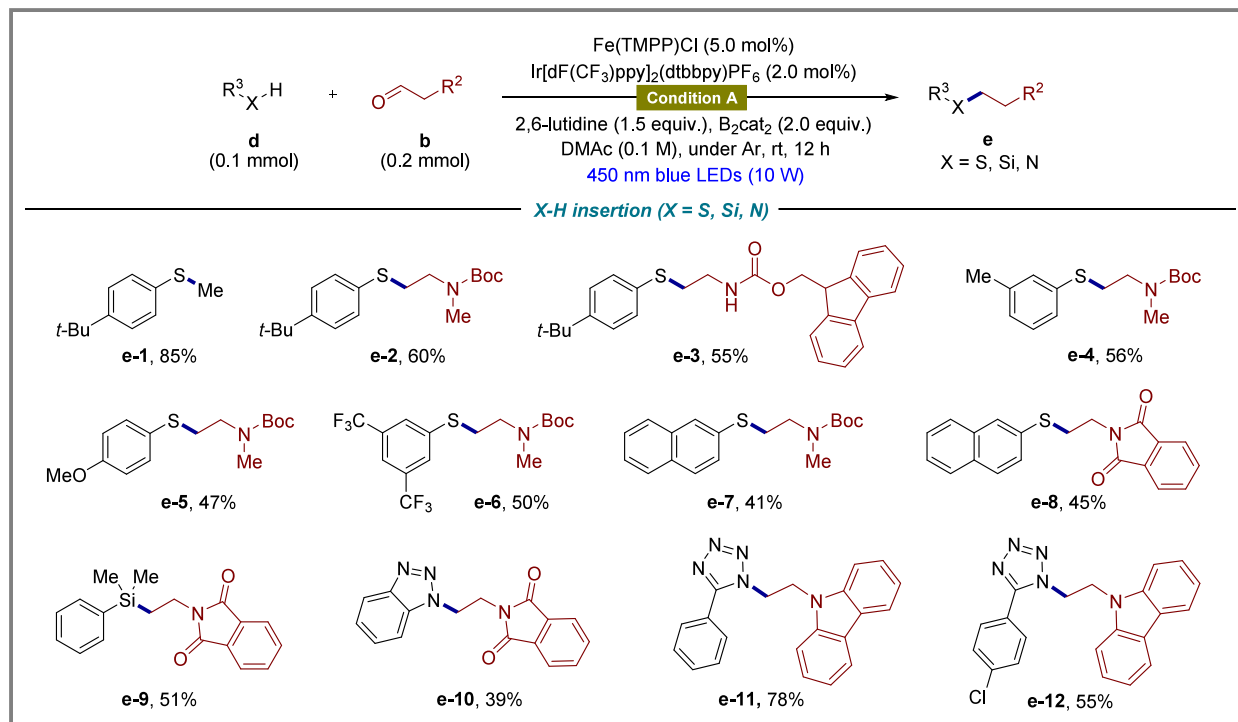
M) at room temperature, under Ar atmosphere, 450 nm LEDs (10 W), 12 h. Conditions C: alkene **a** (0.1 mmol, 1.0 equiv), aldehyde **b** (0.2 mmol, 2.0 equiv), 2,6-lutidine (0.15 mmol, 1.5 equiv),  $B_2cat_2$  (0.2 mmol, 2.0 equiv),  $Fe(TMPP)Cl$  (5.0 mol %) in DMAc:acetone = 1:1 (1.0 mL, 0.1 M) at room temperature, under Ar atmosphere, 390 nm LEDs (10 W), 12 h. Yields of isolated products after chromatographic purification. Diastereomeric ratio (d.r.) determined by  $^1H$  NMR (*trans*:*cis*).

**Substrate Scope.** With optimized conditions established, we explored the generality of this metallaphotoredox-catalyzed cyclopropanation strategy employing the in situ formed nonstabilized carbenes. A diverse array of alkenes, including styrenes,  $\alpha$ -heteroatom-substituted alkenes, disubstituted alkenes, dienes, unactivated alkenes, and electron-deficient alkenes, reacted efficiently with alkyl aldehyde **b** under developed Condition A. Delightfully, this method enables access to a broad spectrum of cyclopropanes from the corresponding alkenes, including previously inaccessible derivatives. As shown in Scheme 1, styrene derivatives bearing both electron-withdrawing groups (**c-2**) and electron-donating groups (**c-4** – **c-6**) exhibited high reaction efficiency and diastereoselectivity (up to 12.5:1 d.r.) to react with benzyloxyacetaldehyde (**b-1**). Notably, the sterically hindered styrene (**c-7**), 2-vinylnaphthalene (**c-8**), 5-vinylindole (**c-9**), and *N*-ethyl-3-vinylcarbazole (**c-10**) were all successfully transformed into the cyclopropane products in high yields and good to moderate *trans*-selectivity. The protocol further accommodated heteroaryl-functionalized styrenes, including thiophene (**c-11**), benzofuran (**c-12**), and indole (**c-13**) derivatives. Moreover, vinyl ferrocene underwent this metallaphotoredox-catalyzed cyclopropanation reaction smoothly to deliver the desired product **c-14** in 81% yield with excellent diastereoselectivity (>20:1 d.r.), highlighting the versatility of this strategy for structurally diverse complex molecules. The reactivity of  $\alpha$ -heteroatom-substituted alkenes was also investigated under the optimized Condition A. To our delight, enol ethers (**c-15** – **c-17**), enamide (**c-18**), and enamine (**c-19**) all participated efficiently in the reaction, yielding the corresponding  $\alpha$ -heteroatom functionalized cyclopropanes, which are a class of structural motifs that commonly exist in bioactive natural products and medicinal scaffolds. The structure of **c-19** was unambiguously determined by X-ray crystallographic analysis (CCDC 2470832), confirming the *trans*-configuration as the predominant form. Furthermore, a steric evaluation of the reaction scope revealed good tolerance for disubstituted alkenes. For example, 1,1-disubstituted styrenes (**c-20** – **c-22**) and vinyl boronate esters (**c-23** – **c-24**) were suitable for this photoinduced transformation. Analogously, the more sterically hindered 1,2-disubstituted alkenes afforded fused bicyclic products **c-25**—structures traditionally challenging to access via conventional methods. In the next series, we shifted our exploration to diverse diene substrates. Simple buta-1,3-diene (**c-26**), monosubstituted dienes (**c-27** – **c-28**), and 1,2-disubstituted dienes (**c-29** – **c-30**) were all efficiently converted to the corresponding allylic cyclopropanes, which serve as versatile precursors for further synthetic applications. It is noteworthy mentioning that this protocol enabled the preparation of cyclopropanes bearing two aliphatic substituents (**c-31** – **c-33**) from unactivated aliphatic alkenes, demonstrating the robust synergy between non-stabilized carbenes and inert alkene substrates under these conditions. Furthermore, electron-deficient alkenes (**c-34** – **c-35**) were also identified as competent carbene acceptors in this photoinduced [2 + 1] cycloaddition reaction.

To further demonstrate the synthetic utility of our metallaphotoredox-catalyzed cyclopropanation strategy, we systematically evaluated its applicability in late-stage functionalization using alkenes derived from commercial pharmaceuticals and natural products. As shown in Scheme 1, our approach provides a versatile platform for constructing diverse cyclopropanes bearing medicinally relevant scaffolds. Naturally derived compounds, including *L*-menthol (**c-37**), citronellol (**c-39**), diprogulic acid (**c-40**), estrone (**c-41**), and citral (**c-42**), underwent successful cyclopropanation with aldehydes, delivering the corresponding cyclopropane products in 55–80% yields and preferential *trans*-selectivity. We further explored the viable terminal alkenes bearing complex pharmaceutical structural motifs to undergo a photocatalytic cyclopropanation reaction. Under the standard Condition A, the use of pharmaceutical derived molecules such as fenofibrate (**c-36**), adapalene (**c-38**), ibuprofen (**c-43**), febuxostat (**c-44**), and oxaprozin (**c-45**), universally delivers the cyclopropane-containing analogs with comparable reaction efficiency and diastereoselectivity.

Having established the metallaphotoredox-catalyzed cyclopropanation of alkenes, we next sought to examine a series of aldehydes to be suitable carbene precursors. As shown in Scheme 2, simple aliphatic aldehydes were first investigated under the optimized Condition A. Formaldehyde (**c-46**), acetaldehyde (**c-47**), 3-phenylpropanal (**c-48**), and 3-phenoxypropanal (**c-49**) readily participated in the photoinduced cyclopropanation reaction, delivering the corresponding products in moderate to good yields. Remarkably, the protocol demonstrated broad functional group compatibility. Halogen-functionalized aldehydes (**c-50**), olefin-containing analogs (**c-51** – **c-52**), hydroxy-substituted aldehyde (**c-53**), and ester-bearing substrate (**c-54**) were all well-tolerated. To our delight, even Boc- and Fmoc-protected amino aldehydes (**c-55** – **c-58**) proved compatible under the optimal conditions, affording the cyclopropanation products. Additionally, aldehydes incorporating isoindoline-1,3-dione (**c-59** – **c-60**) or carbazole (**c-61**) motifs were successfully tolerated, demonstrating the robustness of this methodology.

We next directed our efforts toward generating fluoroalkyl carbenes as key intermediates for the synthesis of high-value fluorinated cyclopropanes. These fluoromethylated carbocycles have gained prominence in medicinal chemistry due to their enhanced metabolic stability and favorable pharmacokinetic/pharmacodynamic properties.<sup>23</sup> However, conventional strategies to access fluoromethylated cyclopropanes remain constrained by reliance on diazo precursors, which introduce significant safety risks associated with their instability and explosive potential.<sup>24</sup> This limitation underscores the critical need for alternative methodologies to bypass hazardous intermediates. Based on the optimized conditions established earlier, we investigated the possibility of trifluoroacetaldehyde hydrate as a fluoroalkyl carbene precursor under the developed metallaphotoredox platform. Unfortunately, application of the previously optimized Condition A failed to yield the desired trifluoromethylated cyclopropanes. Recently, photoredox-cata-

Scheme 3. Substrate Scope of  $\sigma$ -Bond Insertion Reaction<sup>a</sup>

<sup>a</sup>Conditions A: thiol, silane or amine **d** (0.1 mmol, 1.0 equiv), aldehyde **b** (0.2 mmol, 2.0 equiv),  $Ir[dF(CF_3)ppy]_2(dtbbpy)PF_6$  (2.0 mol %), 2,6-lutidine (0.15 mmol, 1.5 equiv),  $B_2cat_2$  (0.2 mmol, 2.0 equiv),  $Fe(TMPP)Cl$  (5.0 mol %) in DMAc (1.0 mL, 0.1 M) at room temperature, under Ar atmosphere, 450 nm LEDs (10 W), 12 h. Yields of isolated products after chromatographic purification.

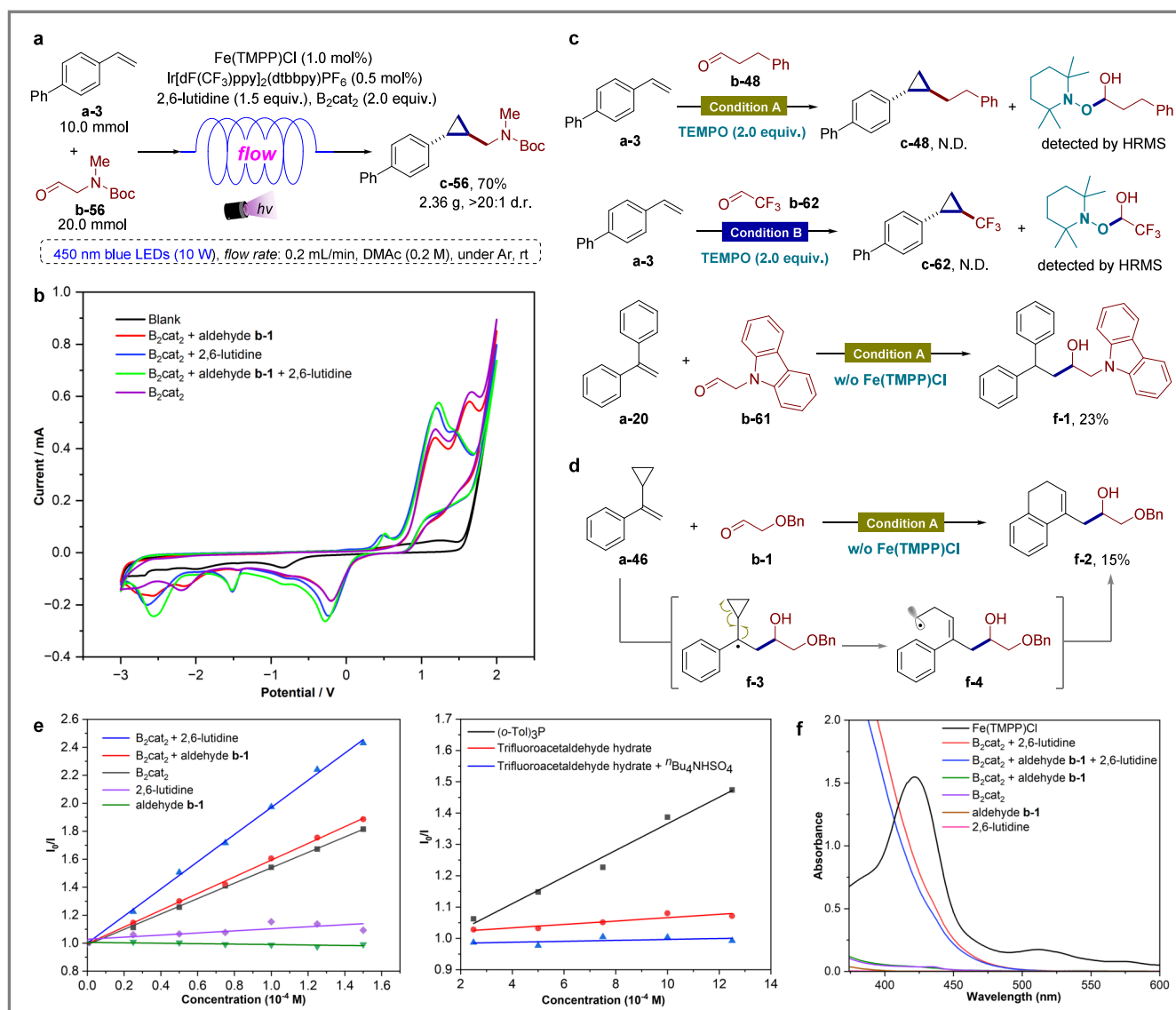
lyzed phosphine-mediated deoxygenation of hexafluoroacetone hydrate has been established as a robust strategy for the generation of ketyl intermediates.<sup>25</sup> We hypothesized that a metallaphotoredox-catalytic system in combination with a phosphine-mediated pathway could enable the utilization of fluoroalkyl carbenes. With the optimal reaction conditions established (Condition B), we explored a diverse array of styrene derivatives (**c-62** – **c-68**) as suitable reaction counterparts, demonstrating high efficiency and excellent diastereoselectivity (>20:1 d.r.) with the carbene species generated from trifluoroacetaldehyde hydrate (Scheme 2). Enamine (**c-69**), vinyl boronate esters (**c-70**) and 1,1-disubstituted styrenes (**c-71** – **c-73**) were all converted into the corresponding trifluoromethyl cyclopropanation products with excellent diastereoselectivity and moderate to good yields. Late-stage modification of complex organic molecules is the basis for the evaluation of a practical protocol. Pharmaceutical scaffolds including fenofibrate (**c-74**) and estrone (**c-75**), along with the terpene derivative *L*-menthol (**c-76**), were smoothly functionalized to afford the corresponding trifluoromethyl cyclopropanes in 51–61% yields and >20:1 diastereomeric ratio.

In the pursuit of sustainable and eco-friendly chemical processes, the research field of photocatalyst-free reactions triggered by visible light irradiation has attracted increasing attention.<sup>26</sup> Under the developed Condition C, which does not involve any photocatalyst, we systematically investigated the substrate scope of structurally diverse alkenes and aldehydes for the photosensitizer-free visible-light-promoted cyclopropanation reaction (Scheme 2). Styrene (**c-10'**), enamine (**c-19'**) and monosubstituted dienes (**c-30'**) were all efficiently converted to the desired cyclopropanic product in moderate

yields under the 390 nm light irradiation. Boc-protected amino aldehyde (**c-55'**) and substrate bearing a carbazole moiety (**c-61'**) were also well accommodated, delivering the corresponding trans-selective cyclopropanes in 58% and 71% yields, respectively.

Beyond its cyclopropanation utility, the Fischer-type carbene character of iron-carbene intermediates enables divergent  $\sigma$ -bond insertion pathways.<sup>27</sup> Building on this concept, we successfully demonstrated the X–H ( $X = S, Si$ , and  $N$ )  $\sigma$ -bond insertion reaction using our metallaphotoredox platform (Scheme 3, Condition A). We observed the successful insertion of alkyl aldehydes into S–H bonds, which allows the synthesis of alkylated thioether products (**e-1** – **e-8**) directly from thiols and aldehydes. Si–H insertion into alkyl silane (**e-9**) occurred smoothly with this metallaphotoredox platform. Furthermore, N–H alkylation of both triazole (**e-10**) and tetrazole (**e-11** – **e-12**) proceeded successfully. The successful demonstration of  $\sigma$ -bond insertion in these diverse settings further shows the ability of carbene intermediates to engage in useful bond formations beyond annulation and establishes their power as reactive intermediates that may be effectively harnessed through our photoinduced radical approach.

**Synthetic Application.** Having established the metallaphotoredox-catalyzed cyclopropanation protocol, we next sought to evaluate its synthetic utility. As illustrated in Figure 2a, a gram-scale continuous-flow reaction was implemented under the irradiation of 450 nm blue LEDs (10 W), facilitating the coupling reaction of styrene derivative (**a-3**) and Boc-protected 2-(methylamino)acetaldehyde (**b-56**) even with a reduced amount of an iridium-based photocatalyst and an iron-porphyrin complex. By applying a flow rate of 0.2 mL·min<sup>−1</sup>



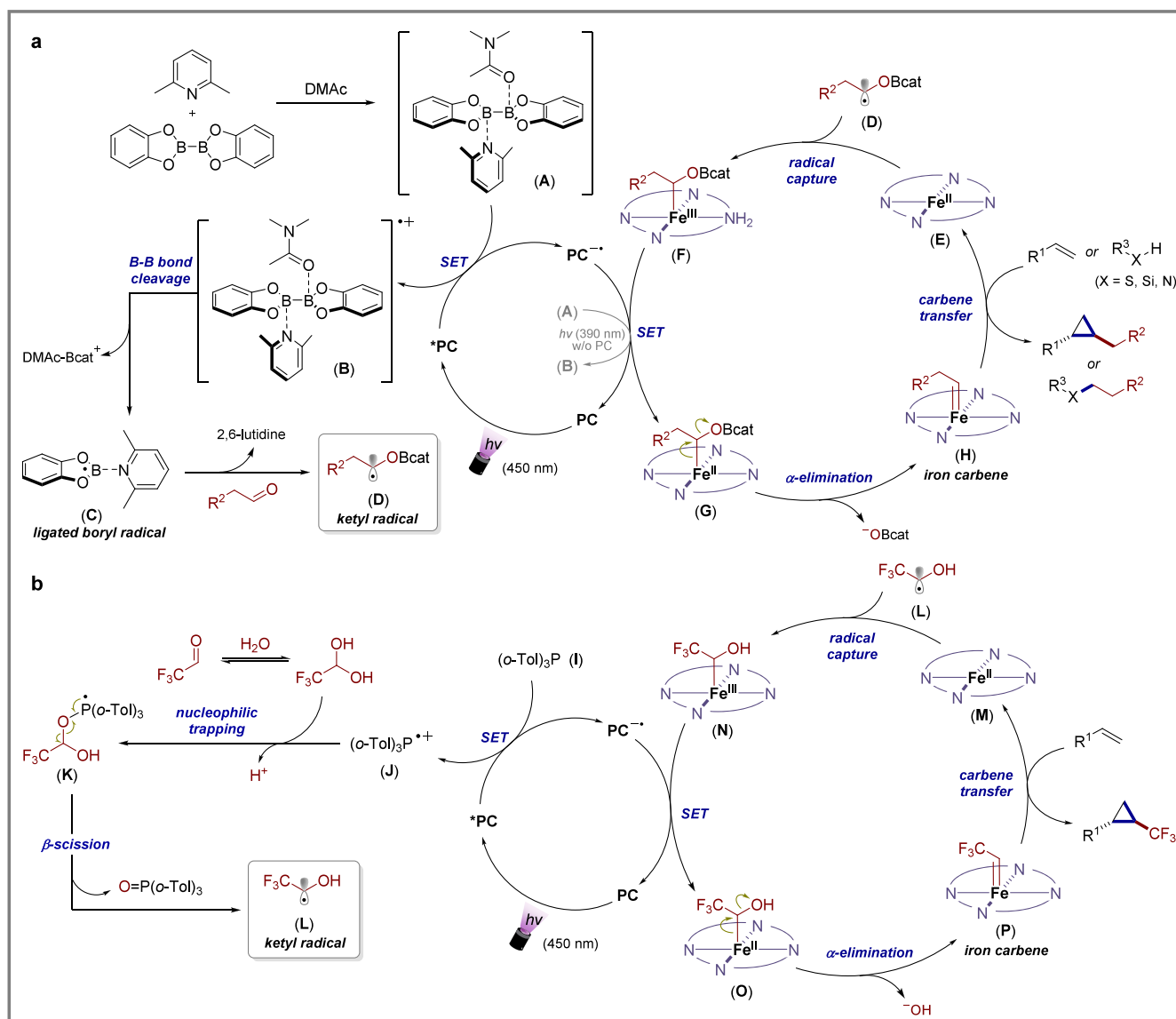
**Figure 2.** Synthetic applications and mechanistic investigations. (a) A gram-scale synthesis in continuous flow. (b) Cyclic voltammetry (CV) studies. Cyclic voltammetry studies were performed in DMAc (10 mL) by using glassy carbon as the working electrode, Pt wire as the counter electrode, and SCE as the reference electrode under Ar at room temperature. Scan rate is 100 mV/s. Black line - 10 mL  $n\text{Bu}_4\text{NBF}_4$  solution (0.1 M); red line -  $\text{B}_2\text{cat}_2$  (20 mM), aldehyde (20 mM), 10 mL  $n\text{Bu}_4\text{NBF}_4$  DMAc solution (0.1 M); blue line -  $\text{B}_2\text{cat}_2$  (20 mM), 2,6-lutidine (15 mM), 10 mL  $n\text{Bu}_4\text{NBF}_4$  DMAc solution (0.1 M); green line -  $\text{B}_2\text{cat}_2$  (20 mM), aldehyde (20 mM), 2,6-lutidine (15 mM), 10 mL  $n\text{Bu}_4\text{NBF}_4$  DMAc solution (0.1 M); purple line -  $\text{B}_2\text{cat}_2$  (20 mM), 10 mL  $n\text{Bu}_4\text{NBF}_4$  DMAc solution (0.1 M). (c) Radical trapping experiments. (d) Radical clock experiments. (e) Stern-Volmer quenching experiments. (f) UV-vis absorption spectra of DMA solutions. Black line -  $\text{Fe}(\text{TMPP})\text{Cl}$  solution ( $1.25 \times 10^{-5}$  M); red line -  $\text{B}_2\text{cat}_2$  (0.2 M), 2,6-lutidine (0.15 M); blue line -  $\text{B}_2\text{cat}_2$  (0.2 M), aldehyde (0.2 M), 2,6-lutidine (0.15 M); green line -  $\text{B}_2\text{cat}_2$  (0.2 M), aldehyde (0.2 M); purple line -  $\text{B}_2\text{cat}_2$  (0.2 M); brown line - aldehyde (0.2 M); pink line - 2,6-lutidine (0.15 M).

and a residence time as short as 5 h, we were able to successfully translate the batch protocol for cyclopropanation into a scalable continuous-flow process and scale up the reaction process by 100-fold. The collected reaction solution, after workup and purification, afforded the corresponding *trans*-cyclopropane product **c-56** in 70% yield (2.36 g) and >20:1 diastereomeric ratio.

**Mechanistic Investigation.** Cyclic voltammetry (CV) studies were performed to probe the interaction between  $\text{B}_2\text{cat}_2$  and 2,6-lutidine in this metallaphotoredox-catalyzed cyclopropanation reaction (Figure 2b). In DMAc solution,  $\text{B}_2\text{cat}_2$  exhibited two distinct oxidation peaks at  $E_p = +1.19$  V and  $+1.67$  V vs SCE (purple line). Strikingly, upon introduction of 2,6-lutidine to the  $\text{B}_2\text{cat}_2$  solution, the original

oxidation peak at  $E_p = +1.67$  V vs SCE vanished, while a new oxidation peak emerged at  $E_p = +0.49$  V vs SCE (blue line). These observations demonstrate a specific interaction between  $\text{B}_2\text{cat}_2$  and 2,6-lutidine. The addition of aldehyde induced no significant changes in the CV profile (red and green lines), indicating no detectable interaction between  $\text{B}_2\text{cat}_2$  and the aldehyde. To further elucidate the reaction mechanism, systematic experimental investigations were conducted. Radical trapping studies employing 2,2,6,6-tetra methylpiperidin-1-oxyl (TEMPO) as a radical scavenger concurrently suppressed the formation of cyclopropanes **c-48** and **c-62** under the standard Conditions A and B, respectively. High-resolution mass spectrometry (HRMS) confirmed the presence of TEMPO-radical adducts, indicating the radical nature of this photo-





**Figure 3.** Proposed reaction mechanism. (a) Photoredox-catalyzed cyclopropanation and  $\sigma$ -bond insertion. (b) Photochemical synthesis of trifluoromethyl cyclopropane.

induced transformation (Figure 2c). Consistent with this observation, the introduction of 1,1-diphenylethylene (**a-20**) with aldehyde **b-61** into the photochemical system in the absence of the iron-porphyrin complex successfully led to the formation of ketyl radical-addition product **f-1** in 23% yield, with no formation of the cyclopropanation product. Additionally, a radical-clock experiment using (1-cyclopropylvinyl)-benzene (**a-46**) under iron-free conditions produced the ring-opening product **f-2** in 15% yield (Figure 2d). The formation of **f-2** was supposed to be achieved through the addition of a ketyl radical species to alkene **a-46** to form intermediate **f-3**, followed by a radical-mediated cyclopropane ring-opening process to generate the terminal alkyl radical species **f-4**. This radical intermediate **f-4** undergoes intramolecular cyclization to form 1,2-dihydronaphthalene product **f-2**. All of these results in radical-trapping and radical-clock experiments suggest that the reaction likely involves the generation of crucial ketyl radical species from the corresponding aldehydes via  $B_2cat_2$ -mediated reduction.

In addition, Stern–Volmer quenching experiments were carried out and are shown in Figure 2e. The observations revealed that the excited-state photocatalyst could be more effectively quenched by the mixture of  $\text{B}_2\text{cat}_2$  and 2,6-lutidine in DMAc, not by the aldehyde substrate. These observations collectively support the generation of a ligated boryl radical via single-electron oxidation of the lutidine-diboron complex.<sup>28</sup> Similarly, the most efficient quenching of the excited photocatalyst under Condition B was achieved by the triarylphosphine reagent. In order to gain further insight into the mechanism of the transformation under photocatalyst-free conditions (Condition C), we began to investigate the formation of an electron-donor–acceptor (EDA) complex between 2,6-lutidine and  $\text{B}_2\text{cat}_2$  by UV/vis absorption spectroscopy.<sup>29</sup> As shown in Figure 2f, when a DMAc solution of 2,6-lutidine was treated with  $\text{B}_2\text{cat}_2$ , a dramatic color change was observed, and this phenomenon was accompanied by a bathochromic shift in the absorption spectrum, which is diagnostic of an EDA complex. Although  $\text{Fe}(\text{TMPP})\text{Cl}$  catalyst also exhibits visible light absorption at both 450 and

390 nm, the control experimental results indicated that Fe(TMPP)Cl did not act as a photocatalyst to carry out single electron transfer process.

On the basis of the above observations, two plausible reaction mechanisms are proposed, as shown in Figure 3. For the photoredox-catalyzed cyclopropanation and  $\sigma$ -bond insertion reactions (Condition A), initiation of photoinduced reaction starts with the formation of complex (A) from 2,6-lutidine, B<sub>2</sub>cat<sub>2</sub>, and DMAc (Figure 3a). Under visible light irradiation ( $\lambda$  = 450–455 nm), the complex (A) could reductively quench the excited photocatalyst (PC\*) to generate the radical cation intermediate (B), while generating the reduced photocatalyst (PC<sup>•-</sup>) (Condition A). Alternatively, in the absence of an external photocatalyst, the in situ generated EDA complex (A) can be effectively photoexcited by purple light ( $\lambda$  = 390–395 nm) to reach the excited intermediate, which could be oxidatively quenched by the iron(III)-porphyrin complex (F) to form the radical cation intermediate (B) and low-valent iron(II) complex (G) (Condition C). Radical cation (B) undergoes boron–boron bond cleavage to generate key pyridine-ligated boryl radical species (C), which would add to the carbonyl group of aldehyde to form ketyl radical species (D). In parallel, precatalyst Fe(TMPP)Cl is reduced from Fe(III) to Fe(II) to generate a reservoir of Fe(TMPP) (E). This iron(II) complex may readily capture the ketyl radical (D), followed by a single-electron transfer (SET) process to release a reduced  $\alpha$ -oxy organoiron species (G) while closing the photocatalytic cycle and regenerating the photocatalyst (PC). The  $\alpha$ -oxy iron(II) complex (G) then undergoes  $\alpha$ -elimination to form a reactive iron carbene intermediate (H) that engages in the sequential cyclopropanation and  $\sigma$ -bond insertion steps, delivering the target products and resetting the iron catalyst to the iron(II) complex (E). In the trifluoromethyl cyclopropanation system (Condition B), the excited photocatalyst (PC\*) was reductively quenched by (*o*-Tol)<sub>3</sub>P via a single electron transfer process, generating the reductive photocatalyst (PC<sup>•-</sup>) species and (*o*-Tol)<sub>3</sub>P<sup>•+</sup> radical cation (J), as shown in Figure 3b. Subsequently, polar nucleophilic trapping of the (*o*-Tol)<sub>3</sub>P<sup>•+</sup> radical cation with deprotonated trifluoroacetaldehyde hydrate formed the phosphoranyl radical (K), which facily underwent  $\beta$ -scission to generate the ketyl radical intermediate (L). Next, this ketyl radical intermediate engages in a synergistic interplay of photoredox and iron catalytic cycles to efficiently construct the trifluoromethyl cyclopropane product.

### 3. CONCLUSION

In summary, we have developed a new metallaphotocatalytic platform that effectively generates alkyl-substituted non-stabilized carbenes through the merger of iron and photoredox dual catalysis. This method achieves the direct use of alkyl aldehydes as carbene precursors in metallaphotoredox catalysis, eliminating the need for substrate prefunctionalization. The reaction is proposed to proceed via a ligated boryl radical addition pathway. Furthermore, this protocol features mild conditions, a broad substrate scope, good functional group tolerance, and step economy. Late-stage modification of structurally complex molecules demonstrates the practicability. Detailed mechanistic studies—including radical trapping experiments, Stern–Volmer quenching, cyclic voltammetry, and UV/vis spectroscopy—support the proposed pathway. We anticipate that this metallaphotocatalytic strategy will serve as a

powerful synthetic tool for carbene generation from feedstock chemicals. Further studies based on this dual catalytic manifold are ongoing in our laboratory.

## ■ ASSOCIATED CONTENT

### Data Availability Statement

The data underlying this study are available in the published article and its Supporting Information.

### Supporting Information

The Supporting Information is available free of charge at <https://pubs.acs.org/doi/10.1021/jacs.5c12677>.

Experimental details, characterization data, and copies of NMR spectra for all novel compounds (PDF)

### Accession Codes

Deposition Number 2470832 contains the supplementary crystallographic data for this paper. These data can be obtained free of charge via the joint Cambridge Crystallographic Data Centre (CCDC) and Fachinformationszentrum Karlsruhe Access Structures service.

## ■ AUTHOR INFORMATION

### Corresponding Author

Lin Guo – State Key Lab of Urban Water Resource and Environment, Harbin Institute of Technology (Shenzhen), Shenzhen 518055, China; [orcid.org/0000-0002-2398-0684](https://orcid.org/0000-0002-2398-0684); Email: [guolin@hit.edu.cn](mailto:guolin@hit.edu.cn)

### Authors

Rong-Bin Liang – State Key Lab of Urban Water Resource and Environment, Harbin Institute of Technology (Shenzhen), Shenzhen 518055, China

Chao Yang – State Key Lab of Urban Water Resource and Environment, Harbin Institute of Technology (Shenzhen), Shenzhen 518055, China; [orcid.org/0000-0003-1103-0056](https://orcid.org/0000-0003-1103-0056)

Wujiong Xia – State Key Lab of Urban Water Resource and Environment, Harbin Institute of Technology (Shenzhen), Shenzhen 518055, China; School of Chemistry and Chemical Engineering, Henan Normal University, Xinxiang, Henan 453007, China; [orcid.org/0000-0001-9396-9520](https://orcid.org/0000-0001-9396-9520)

Complete contact information is available at: <https://pubs.acs.org/10.1021/jacs.5c12677>

### Notes

The authors declare no competing financial interest.

## ■ ACKNOWLEDGMENTS

We are grateful for the financial support from the National Natural Science Foundation of China (No. 22471049), the Science and Technology Plan of Shenzhen (Nos. JCYJ202-30807094408017, JCYJ20220531095016036, and GXWD-20220817131550002). The project is also supported by State Key Laboratory of Urban-rural Water Resources and Environment (Harbin Institute of Technology) (No. 2025DX15) and the Open Research Fund of the School of Chemistry and Chemical Engineering, Henan Normal University.

## ■ REFERENCES

- (1) (a) Sun, M.-R.; Li, H.-L.; Ba, M.-Y.; Cheng, W.; Zhu, H.-L.; Duan, Y.-T. Cyclopropyl Scaffold: A Generalist for Marketed Drugs. *Mini-Rev. Med. Chem.* **2021**, *21*, 150–170. (b) Shearer, J.; Castro, J.

L.; Lawson, A. D.; MacCoss, M.; Taylor, R. D. Rings in Clinical Trials and Drugs: Present and Future. *J. Med. Chem.* **2022**, *65*, 8699–8712.

(2) (a) Talele, T. T. The “Cyclopropyl Fragment” Is a Versatile Player That Frequently Appears in Preclinical/Clinical Drug Molecules. *J. Med. Chem.* **2016**, *59*, 8712–8756. (b) Lovering, F.; Bikker, J.; Humblet, C. Escape from flatland: Increasing saturation as an approach to improving clinical success. *J. Med. Chem.* **2009**, *52*, 6752–6756.

(3) (a) Ebner, C.; Carreira, E. M. Cyclopropanation Strategies in Recent Total Syntheses. *Chem. Rev.* **2017**, *117*, 11651–11679. (b) Lebel, H.; Marcoux, J.-F.; Molinaro, C.; Charette, A. B. Stereoselective Cyclopropanation Reactions. *Chem. Rev.* **2003**, *103*, 977–1050. (c) Wu, W.; Lin, Z.; Jiang, H. Recent advances in the synthesis of cyclopropanes. *Org. Biomol. Chem.* **2018**, *16*, 7315–7329. (d) Chen, Z. L.; Xie, Y.; Xuan, J. Visible Light-Mediated Cyclopropanation: Recent Progress. *Eur. J. Org. Chem.* **2022**, *2022*, No. e202201066.

(4) Green, S. P.; Wheelhouse, K. M.; Payne, A. D.; Hallett, J. P.; Miller, P. W.; Bull, J. A. Thermal Stability and Explosive Hazard Assessment of Diazo Compounds and Diazo Transfer Reagents. *Org. Process Res. Dev.* **2020**, *24*, 67–84.

(5) (a) Ford, A.; Miel, H.; Ring, A.; Slattery, C. N.; Maguire, A. R.; McKerver, M. A. Modern Organic Synthesis with  $\alpha$ -Diazocarbonyl Compounds. *Chem. Rev.* **2015**, *115*, 9981–10080. (b) Zhu, D.; Chen, L.; Fan, H.; Yao, Q.; Zhu, S. Recent progress on donor and donor-donor carbenes. *Chem. Soc. Rev.* **2020**, *49*, 908–950. (c) Lindsay, V. N.; Nicolas, C.; Charette, A. B. Asymmetric Rh(II)-Catalyzed Cyclopropanation of Alkenes with Diaceptor Diazo Compounds: P-Methoxyphenyl Ketone as a General Stereoselectivity Controlling Group. *J. Am. Chem. Soc.* **2011**, *133*, 8972–8981.

(6) Morandi, B.; Carreira, E. M. Iron-catalyzed cyclopropanation in 6 M KOH with in situ generation of diazomethane. *Science* **2012**, *335*, 1471–1474.

(7) (a) Proctor, L. D.; Warr, A. J. Development of a continuous process for the industrial generation of diazomethane. *Org. Process Res. Dev.* **2002**, *6*, 884–892. (b) Rullière, P.; Benoit, G.; Allouche, E. M.; Charette, A. B. Safe and Facile Access to Nonstabilized Diazoalkanes Using Continuous Flow Technology. *Angew. Chem., Int. Ed.* **2018**, *57*, 5777–5782. (c) Hatridge, T. A.; Wei, B.; Davies, H. M.; Jones, C. W. Copper-Catalyzed, Aerobic Oxidation of Hydrazone in a Three-Phase Packed Bed Reactor. *Org. Process Res. Dev.* **2021**, *25*, 1911–1922.

(8) (a) Berger, K. E.; Martinez, R. J.; Zhou, J.; Uyeda, C. Catalytic Asymmetric Cyclopropanations with Nonstabilized Carbenes. *J. Am. Chem. Soc.* **2023**, *145*, 9441–9447. (b) Uyeda, C.; Kalb, A. E. Catalytic Reductive Carbene Transfer Reactions. *Chem. Catal.* **2022**, *2*, 667–678. (c) Werth, J.; Berger, K.; Uyeda, C. Cobalt Catalyzed Reductive Spirocyclopropanation Reactions. *Adv. Synth. Catal.* **2020**, *362*, 348–352. (d) Werth, J.; Uyeda, C. Cobalt-Catalyzed Reductive Dimethylcyclopropanation of 1, 3-Dienes. *Angew. Chem., Int. Ed.* **2018**, *130*, 14098–14102. (e) Werth, J.; Uyeda, C. Regioselective Simmons-Smith-Type Cyclopropanations of Polyalkenes Enabled by Transition Metal Catalysis. *Chem. Sci.* **2018**, *9*, 1604–1609. (f) Cai, B.-G.; Empel, C.; Jana, S.; Xuan, J.; Koenigs, R. M. Catalytic Olefin Cyclopropanation with in Situ-Generated Dialkyl Diazomethanes Via Co(II)-Based Metalloradical Catalysis. *ACS Catal.* **2023**, *13*, 11851–11856. (g) Johnson, J. D.; Teeple, C. R.; Akkawi, N. R.; Wilkerson-Hill, S. M. Efficient Synthesis of Orphaned Cyclopropanes Using Sulfones as Carbene Equivalents. *J. Am. Chem. Soc.* **2022**, *144*, 14471–14476. (h) del Hoyo, A. M.; Herraiz, A. G.; Suero, M. G. A Stereoconvergent Cyclopropanation Reaction of Styrenes. *Angew. Chem., Int. Ed.* **2017**, *56*, 1610–1613. (i) Phelan, J. P.; Lang, S. B.; Compton, J. S.; Kelly, C. B.; Dykstra, R.; Gutierrez, O.; Molander, G. A. Redox-Neutral Photocatalytic Cyclopropanation via Radical/Polar Crossover. *J. Am. Chem. Soc.* **2018**, *140*, 8037–8047. (j) Ji, C.-L.; Han, J.; Li, T.; Zhao, C.-G.; Zhu, C.; Xie, J. Photoinduced gold-catalyzed divergent dechloroalkylation of gem-dichloroalkanes. *Nat. Catal.* **2022**, *5*, 1098–1109. (k) Teye-Kau, J. H. G.; Ayodele, M. J.; Pitre, S. P. Vitamin B12-Photocatalyzed Cyclopropanation of Electron-Deficient Alkenes Using Dichloromethane as the Methylene

Source. *Angew. Chem., Int. Ed.* **2024**, *63*, No. e202316064. (l) Aragón, J.; Sun, S.; Fernández, S.; Lloret-Fillol, J. Dichloromethane as C1 Synthon for the Photoredox Catalytic Cyclopropanation of Aromatic Olefins. *Angew. Chem., Int. Ed.* **2024**, *63*, No. e202405580. (m) Ni, S.; Spinnato, D.; Cornella, J. Reductive Cyclopropanation through Bismuth Photocatalysis. *J. Am. Chem. Soc.* **2024**, *146*, 22140–22144.

(9) Yang, W. C.; Feng, J. G.; Wu, L.; Zhang, Y. Q. Aliphatic Aldehydes: Novel Radical Alkylating Reagents. *Adv. Synth. Catal.* **2019**, *361*, 1700–1709.

(10) (a) Zhang, L.; DeMuynck, B. M.; Paneque, A. N.; Rutherford, J. E.; Nagib, D. A. Carbene Reactivity from Alkyl and Aryl Aldehydes. *Science* **2022**, *377*, 649–654. (b) Zhang, L.; Nagib, D. A. Carbonyl cross-metathesis via deoxygenative gem-di-metal catalysis. *Nat. Chem.* **2024**, *16*, 107–113. (c) DeMuynck, B. M.; Zhang, L.; Ralph, E. K.; Nagib, D. A. Cyclopropanation of Unactivated Alkenes with Non-Stabilized Iron Carbenes. *Chem.* **2024**, *10*, 1015–1027. (d) Ngo, D. T.; Garwood, J. J.; Nagib, D. A. Cyclopropanation with Non-Stabilized Carbenes Via Ketyl Radicals. *J. Am. Chem. Soc.* **2024**, *146*, 24009–24015.

(11) (a) Prier, C. K.; Rankic, D. A.; MacMillan, D. W. C. Visible light photoredox catalysis with transition metal complexes: applications in organic synthesis. *Chem. Rev.* **2013**, *113*, 5322–5363. (b) Shaw, M. H.; Twilton, J.; MacMillan, D. W. Photoredox catalysis in organic chemistry. *J. Org. Chem.* **2016**, *81*, 6898–6926. (c) Skubi, K. L.; Blum, T. R.; Yoon, T. P. Dual catalysis strategies in photochemical synthesis. *Chem. Rev.* **2016**, *116*, 10035–10074. (d) Romero, N. A.; Nicewicz, D. A. Organic photoredox catalysis. *Chem. Rev.* **2016**, *116*, 10075–10166.

(12) (a) Péter, Á.; Agasti, S.; Knowles, O.; Pye, E.; Procter, D. J. Recent advances in the chemistry of ketyl radicals. *Chem. Soc. Rev.* **2021**, *50*, 5349–5365. (b) Lee, K. N.; Ngai, M.-Y. Recent Developments in Transition-Metal Photoredox-Catalyzed Reactions of Carbonyl Derivatives. *Chem. Commun.* **2017**, *53*, 13093–13112. (c) Xia, Q.; Dong, J.; Song, H.; Wang, Q. Visible-Light Photocatalysis of the Ketyl Radical Coupling Reaction. *Chem.—Eur. J.* **2019**, *25*, 2949–2961.

(13) (a) Tarantino, K. T.; Liu, P.; Knowles, R. R. Catalytic Ketyl-Olefin Cyclizations Enabled by Proton-Coupled Electron Transfer. *J. Am. Chem. Soc.* **2013**, *135*, 10022–10025. (b) Rono, L. J.; Yayla, H. G.; Wang, D. Y.; Armstrong, M. F.; Knowles, R. R. Enantioselective Photoredox Catalysis Enabled by Proton-Coupled Electron Transfer: Development of an Asymmetric Aza-Pinacol Cyclization. *J. Am. Chem. Soc.* **2013**, *135*, 17735–17738. (c) Nakajima, M.; Fava, E.; Loescher, S.; Jiang, Z.; Rueping, M. Photoredox-Catalyzed Reductive Coupling of Aldehydes, Ketones, and Imines with Visible Light. *Angew. Chem., Int. Ed.* **2015**, *54*, 8828–8832. (d) Lee, K. N.; Lei, Z.; Ngai, M.-Y.  $\beta$ -Selective Reductive Coupling of Alkenylpyridines with Aldehydes and Imines Via Synergistic Lewis Acid/Photoredox Catalysis. *J. Am. Chem. Soc.* **2017**, *139*, 5003–5006. (e) Cao, K.; Tan, S. M.; Lee, R.; Yang, S.; Jia, H.; Zhao, X.; Qiao, B.; Jiang, Z. Catalytic Enantioselective Addition of Prochiral Radicals to Vinylpyridines. *J. Am. Chem. Soc.* **2019**, *141*, 5437–5443.

(14) (a) Ischay, M. A.; Anzovino, M. E.; Du, J.; Yoon, T. P. Efficient Visible Light Photocatalysis of [2 + 2] Enone Cycloadditions. *J. Am. Chem. Soc.* **2008**, *130*, 12886–12887. (b) Petronijević, F. R.; Nappi, M.; MacMillan, D. W. C. Direct  $\beta$ -Functionalization of Cyclic Ketones with Aryl Ketones Via the Merger of Photoredox and Organocatalysis. *J. Am. Chem. Soc.* **2013**, *135*, 18323–18326. (c) Du, J.; Skubi, K. L.; Schultz, D. M.; Yoon, T. P. A Dual-Catalysis Approach to Enantioselective [2 + 2] Photocycloadditions Using Visible Light. *Science* **2014**, *344*, 392–396. (d) Tanaka, K., III Ketyl Radical Generation by Photoexcited Palladium and Development of Organopalladium-Type Reactions. *ACS Catal.* **2024**, *14*, 5269–5274. (e) Chi, Z.; Liao, J.-B.; Cheng, X.; Ye, Z.; Yuan, W.; Lin, Y.-M.; Gong, L. Asymmetric Cross-Coupling of Aldehydes with Diverse Carbonyl or Iminyl Compounds by Photoredox-Mediated Cobalt Catalysis. *J. Am. Chem. Soc.* **2024**, *146*, 10857–10867.

(15) Roth, H. G.; Romero, N. A.; Nicewicz, D. A. Experimental and Calculated Electrochemical Potentials of Common Organic Molecules



for Applications to Single-Electron Redox Chemistry. *Synlett* **2016**, 27, 714–723.

(16) Zhang, L.; Zhou, F.-Y.; Jiao, L. N-Boryl Pyridyl Anion Chemistry. *Acc. Chem. Res.* **2025**, 58, 1023–1035.

(17) (a) Wang, G.; Cao, J.; Gao, L.; Chen, W.; Huang, W.; Cheng, X.; Li, S. Metal-Free Synthesis of C-4 Substituted Pyridine Derivatives Using Pyridine-Boryl Radicals Via a Radical Addition/Coupling Mechanism: A Combined Computational and Experimental Study. *J. Am. Chem. Soc.* **2017**, 139, 3904–3910. (b) Cao, J.; Wang, G.; Gao, L.; Cheng, X.; Li, S. Organocatalytic reductive coupling of aldehydes with 1,1-diarylethylenes using an in situ generated pyridine-boryl radical. *Chem. Sci.* **2018**, 9, 3664–3671.

(18) Chan, A. Y.; Perry, I. B.; Bissonnette, N. B.; Buksh, B. F.; Edwards, G. A.; Frye, L. I.; Garry, O. L.; Lavagnino, M. N.; Li, B. X.; Liang, Y. Metallaphotoredox: the merger of photoredox and transition metal catalysis. *Chem. Rev.* **2022**, 122, 1485–1542.

(19) (a) Boyle, B. T.; Dow, N. W.; Kelly, C. B.; Bryan, M. C.; MacMillan, D. W. Unlocking carbene reactivity by metallaphotoredox  $\alpha$ -elimination. *Nature* **2024**, 631, 789–795. (b) Vargas, R. M.; Theys, R. D.; Hossain, M. M. A new reaction for the synthesis of carbene precursors from aldehydes and  $C_p(CO)_2Fe-M^+$  ( $M$  = sodium, potassium). *J. Am. Chem. Soc.* **1992**, 114, 777–778. (c) Goswami, M.; de Bruin, B.; Dzik, W. I. Difluorocarbene transfer from a cobalt complex to an electron-deficient alkene. *Chem. Commun.* **2017**, 53, 4382–4385. (d) Brault, D.; Neta, P. Reactions of iron porphyrins with trifluoromethyl, trifluoromethylperoxy, and tribromomethylperoxy radicals. *J. Phys. Chem.* **1987**, 91, 4156–4160.

(20) (a) Zhang, L.; Jiao, L. Visible-Light-Induced Organocatalytic Borylation of Aryl Chlorides. *J. Am. Chem. Soc.* **2019**, 141, 9124–9128. (b) Zhang, L.; Wu, Z. Q.; Jiao, L. Photoinduced Radical Borylation of Alkyl Bromides Catalyzed by 4-Phenylpyridine. *Angew. Chem., Int. Ed.* **2020**, 132, 2111–2115.

(21) (a) Hamaker, C. G.; Mirafzal, G. A.; Woo, L. K. Catalytic Cyclopropanation with Iron(II) Complexes. *Organometallics* **2001**, 20, 5171–5176. (b) Ma, C.; Wang, S.; Sheng, Y.; Zhao, X.-L.; Xing, D.; Hu, W. Synthesis and Characterization of Donor-Acceptor Iron Porphyrin Carbenes and Their Reactivities in N-H Insertion and Related Three-Component Reaction. *J. Am. Chem. Soc.* **2023**, 145, 4934–4939. (c) Hock, K. J.; Knorrscheidt, A.; Hommelsheim, R.; Ho, J.; Weissenborn, M. J.; Koenigs, R. M. Tryptamine Synthesis by Iron Porphyrin Catalyzed C–H Functionalization of Indoles with Diazoacetone. *Angew. Chem., Int. Ed.* **2019**, 58, 3630–3634. (d) Empel, C.; Jana, S.; Koenigs, R. M. C-H Functionalization via Iron-Catalyzed Carbene-Transfer Reactions. *Molecules* **2020**, 25, 880–895.

(22) (a) Wu, J.; Bär, R. M.; Guo, L.; Noble, A.; Aggarwal, V. K. Photoinduced Deoxygenative Borylations of Aliphatic Alcohols. *Angew. Chem., Int. Ed.* **2019**, 58, 18830–18834. (b) Wu, J.; Wang, H.; Fang, H.; Wang, K. C.; Ghosh, D.; Fasano, V.; Noble, A.; Aggarwal, V. K. Persistent Boryl Radicals as Highly Reducing Photoredox Catalysts for Debrominative Borylations. *J. Am. Chem. Soc.* **2025**, 147, 19450–19457. (c) Yin, L.; Huang, G.; Lin, X.; Song, X.; Chen, Y.; Yan, T.; Li, M.; Dang, L. Visible light induced boryl radical and its application in reduction of unsaturated X–O ( $X = C, N, S$ ) bonds. *Org. Chem. Front.* **2023**, 10, 4623–4630.

(23) (a) Grygorenko, O. O.; Artamonov, O. S.; Komarov, I. V.; Mykhailiuk, P. K. Trifluoromethyl-substituted cyclopropanes. *Tetrahedron* **2011**, 67, 803–823. (b) Wu, W. F.; Lin, J. H.; Xiao, J. C.; Cao, Y. C.; Ma, Y. Recent advances in the synthesis of  $CF_3$ - or  $HCF_2$ -substituted cyclopropanes. *Asian J. Org. Chem.* **2021**, 10, 485–495.

(24) (a) Deadman, B. J.; Collins, S. G.; Maguire, A. R. Taming hazardous chemistry in flow: the continuous processing of diazo and diazonium compounds. *Chem.—Eur. J.* **2015**, 21, 2298–2308. (b) Mykhailiuk, P. K. 2,2,2-Trifluorodiazoethane ( $CF_3CHN_2$ ): a long journey since 1943. *Chem. Rev.* **2020**, 120, 12718–12755.

(25) Xie, Z. Z.; Zheng, Y.; Yuan, C. P.; Guan, J. P.; Ye, Z. P.; Xiao, J. A.; Xiang, H. Y.; Chen, K.; Chen, X. Q.; Yang, H. Photoredox-Catalyzed Deoxygenation of Hexafluoroacetone Hydrate Enables

Hydroxypolyfluoroalkylation of Alkenes. *Angew. Chem., Int. Ed.* **2022**, 134, No. e20211035.

(26) (a) Candish, L.; Teders, M.; Glorius, F. Transition-Metal-Free, Visible-Light-Enabled Decarboxylative Borylation of Aryl N-Hydroxyphthalimide Esters. *J. Am. Chem. Soc.* **2017**, 139, 7440–7443. (b) Cheng, Y.; Mück-Lichtenfeld, C.; Studer, A. Metal-Free Radical Borylation of Alkyl and Aryl Iodides. *Angew. Chem., Int. Ed.* **2018**, 130, 17074–17078. (c) Fawcett, A.; Pradeilles, J.; Wang, Y.; Mutsuga, T.; Myers, E. L.; Aggarwal, V. K. Photoinduced Decarboxylative Borylation of Carboxylic Acids. *Science* **2017**, 357, 283–286. (d) Shu, C.; Noble, A.; Aggarwal, V. K. Metal-free photoinduced  $C(sp^3)$ -H borylation of alkanes. *Nature* **2020**, 586, 714–719. (e) Almagambetova, K.; Murugesan, K.; Rueping, M. Transition-Metal and Photocatalyst-Free, Redox-Neutral Heteroarylation of  $C(sp^3)$ -H Bonds. *ACS Catal.* **2024**, 14, 12664–12670. (f) Liu, T.; Li, T.; Tea, Z. Y.; Wang, C.; Shen, T.; Lei, Z.; Chen, X.; Zhang, W.; Wu, J. Modular assembly of arenes, ethylene and heteroarenes for the synthesis of 1,2-arylheteroaryl ethanes. *Nat. Chem.* **2024**, 16, 1705–1714. (g) Yu, J.; Zhang, X.; Wu, X.; Liu, T.; Zhang, Z.-Q.; Wu, J.; Zhu, C. Metal-free radical difunctionalization of ethylene. *Chem.* **2023**, 9, 472–482.

(27) Doetz, K. H.; Stendel, J., Jr Fischer carbene complexes in organic synthesis: metal-assisted and metal-templated reactions. *Chem. Rev.* **2009**, 109, 3227–3274.

(28) Liang, R.-B.; Miao, T.-T.; Li, X.-R.; Huang, J.-B.; Ni, S.-F.; Li, S.; Tong, Q.-X.; Zhong, J.-J. Modular assembly of amines and diborons with photocatalysis enabled halogen atom transfer of organohalides for  $C(sp^3)$ – $C(sp^3)$  bond formation. *Chem. Sci.* **2025**, 16, 3580–3587.

(29) Wu, J.; He, L.; Noble, A.; Aggarwal, V. K. Photoinduced Deaminative Borylation of Alkylamines. *J. Am. Chem. Soc.* **2018**, 140, 10700–10704.



CAS BIOFINDER DISCOVERY PLATFORM™

**CAS BIOFINDER  
HELPS YOU FIND  
YOUR NEXT  
BREAKTHROUGH  
FASTER**

Navigate pathways, targets, and  
diseases with precision

Explore CAS BioFinder

**CAS**  
A Division of the  
American Chemical Society